Impact of Mo and Ce on growth of single-walled carbon nanotubes by chemical vapour deposition using MgO-supported Fe catalysts

Cite as:
El-Hendawy, A. N. A., Andrews, R. J., & Alexander, A. J. (2009). Impact of Mo and Ce on growth of single-walled carbon nanotubes by chemical vapour deposition using MgO-supported Fe catalysts. *Applied Surface Science*, 255(16), 7446-7450.

Manuscript received: 26/01/2009; Accepted: 04/04/2009; Article published: 11/04/2009

Impact of Mo and Ce on growth of single-walled carbon nanotubes by chemical vapour deposition using MgO-supported Fe catalysts**

Abdel-Nasser A. El-Hendawy,[1,*] Robert J. Andrews[2] and Andrew J. Alexander[2]

[1]Physical Chemistry Department, National Research Center, 12622 Dokki, Cairo, Egypt.

[2]School of Chemistry, Joseph Black Building, University of Edinburgh, West Mains Road, Edinburgh, EH9 3JJ, UK.

[*]Corresponding author; e-mail: elhendawy@yahoo.com ; tel.: +20 50 223 2515; fax: +20 2 33370931.

[**]Drs Alexander and Andrews thank the UK EPSRC and The Royal Society for financial support of this work. The authors thank Dr Gavin Forrest for useful discussions. Dr El-Hendawy gratefully acknowledges the Egyptian Government for an international visiting fellowship.

Keywords:
Carbon nanotubes, Chemical vapour deposition

Abstract

A series of nine catalysts containing Ce/Fe and Mo/Fe at various loadings on MgO supports have been studied as catalysts for chemical vapour deposition of single-walled carbon nanotubes (SWCNTs) using a methane carbon source. Our results show that the Ce/Fe system is very suitable as a catalyst that favours SWCNT growth, and we question the special importance that has been attributed to Mo as an additive to Fe-based catalysts for SWCNT growth, as it appears that Ce is equally effective. Our results indicate that dehydroaromatization is not a defining step for the growth mechanism, as has been suggested for Mo/Fe systems previously, and show that Ce and Mo do not seriously perturb the well-known Fe/MgO system for growth of high quality SWCNT. Using Raman spectroscopy, we have shown that the Ce/Fe/MgO catalyst system favours growth of SWCNTs with a different distribution of chiralities compared to the analogous Mo/Fe/MgO system.

1. Introduction

The growth of multi-walled carbon nanotubes (MWCNTs) and single-walled carbon nanotubes (SWCNTs) using chemical vapour deposition (CVD) at high temperatures is a well-established technique [1]. The method generally requires the use of a transition metal catalyst, typically Ni, Fe, or Co, which is deposited onto a high surface-area support, such as alumina (Al_2O_3) or aluminosilicate (e.g., zeolite Y) [2]. The main advantages of the CVD technique are its simplicity, high throughput, and low running costs. However, there remain several disadvantages to CVD, e.g., it is still very challenging to produce SWCNTs in high yields and with high quality. SWCNTs are very highly strained structures, and are therefore less abundant in the synthesized products. Large-volume growth of SWCNTs is an important goal because they exhibit the sought-after features of the carbon nanotube, such as high electrical conductivity and enormous tensile strength [3].

It has been found that bimetallic catalysts are much more effective for CVD growth of SWCNTs than single metals. Combinations that have been used successfully include Rh/Pd, Ni/Co, Ni/Y, and Ni/La. In particular, it has been found that addition of small proportions (< 10%) of Mo into Fe-based catalysts can increase both the quality and the yield of SWCNTs [4]. There may be a number of factors that influence the behaviour of the bimetallic catalyst. It is generally accepted that metal nanoparticles are formed at the high temperatures of the CVD process, and that these nanoparticles act as templates for the growth of the SWCNTs. It is believed that a small amount of Mo dissolved into the Fe nanoparticle helps to lower the melting point of the particle, thus stimulating activity of the catalyst. A popular mechanism that has been proposed for the growth of SWCNTs is the *decomposition mechanism*, in which the carbon precursor, such as methane, decomposes to elemental C that is stored by the metal nanoparticle, and is then released to produce the hexagonal nanotube network [2]. There is

substantial evidence to support decomposition, and it has been postulated that formation of metal carbides are an important feature of this mechanism [5]. The presence of Mo in the Fe nanoparticle could not only lower its melting point, but also increase the solubility of C in the nanoparticle [5].

Another explanation of the growth mechanism comes from noting the use of zeolite-supported Mo as an effective catalyst for dehydroaromatization (DHA) of methane [6]. In the *ring-addition mechanism* of SWCNT growth, it is postulated that growth of the nanotube occurs by addition of the six-membered rings that produce the graphitic structure. Evidence for this mechanism comes from analysis of H_2 gas in the exhaust of CVD experiments run with benzene as the carbon source [7,8]. Therefore, it is suggested that the DHA activity of the Mo in the Fe-based catalyst could produce carbon rings from methane that may then take part in the ring-addition process.

The importance of the support in CVD of SWCNTs has often been ignored in favour of studying the effects of the composition of the metal catalyst. In particular, there have been very few studies of MgO as a catalyst support, in spite of the fact that it is relatively cheap and obtainable commercially as a nanopowder. Also, MgO has the critical advantage that it can be easily removed and recycled after the CVD using dilute acid: by comparison, removal of aluminosilicates requires harsher treatments, such as concentrated acids [9]. The Fe/MgO catalyst has been shown to be a highly effective combination for SWCNT growth [9-15], even without the use of a bimetallic catalyst. The reason for the success of Fe/MgO has been shown to be due to the strong interaction between well-dispersed Fe nanoparticles and the MgO support. In particular, there is evidence that the MgO acts like a sponge, soaking up excess Fe [16]. Once the catalyst has been annealed at high temperature to form a homogeneous solid solution of $MgFe_2O_4$ in MgO, reduction by the carbon-containing gas (e.g., methane) precipitates out very small particles of iron [10].

In the present work, we compare the use of Ce and Mo as components in MgO-supported Fe catalysts for CVD growth of SWCNTs. The use of Ce as a catalyst for growth of CNT by CVD is, to the best of our knowledge, demonstrated here for the first time. We show that small loadings of Mo and Ce are entirely compatible with the Fe/MgO system, and that both Mo and Ce improve the total yield of product while retaining the quality of the SWCNTs produced.

2. Experimental methods

2.1. Catalyst preparation

A series of nine catalysts containing varying proportions of Fe, Mo and Ce salts were prepared. The Fe, Mo and Ce salts used were $Fe(NO_3)_3.9H_2O$, $Ce(NO_3)_3.6H_2O$ and $(NH_4)_2MoO_4$ (ACS grade, Sigma Aldrich, UK). The salts were ground finely and added to dry MgO oxide nanopowder (Sigma Aldrich,

UK) according to the ratios shown in Table 1. The total ratio of metal to MgO support was adjusted to be 28 mol. %. The powdered mixture was immersed in the least amount of deionized water and was then stirred for 20 minutes, followed by ultrasonication in a bath for 10 minutes, until a homogeneous slurry was formed. The slurry was dried at 80 ^{o}C overnight and ground into a fine powder.

Sample label	**% Fe**	**% Mo**	**% Ce**
Fe100	100	0	0
Mo100	0	100	0
Ce100	0	0	100
Ce10	90	0	10
Ce50	50	0	50
Ce90	10	0	90
Mo10	90	10	0
Mo50	50	50	0
Mo90	10	90	0

Table 1. Summary of the catalyst samples studied in the present work, showing relative proportions of metal in each catalyst. The support material in each case was MgO nanopowder, and the loading of total metal was adjusted to be 28 mol. % with respect to the MgO support.

The powdered catalyst (0.1 g) was dispersed into an alumina boat for each experiment. The boat was introduced into the centre of the alumina work tube (25.4 mm diameter) of a furnace (MTF 12/38/250, Carbolite, UK). Gas-tight ends were attached that were connected to the gas handling system. The furnace was heated up to the reaction temperature (900 °C) at a rate of 30 °C min^{-1} in a flow of Ar gas at a rate of 400 cm^3 min^{-1}. Once the furnace had reached the reaction temperature, the gas flow was changed to 200 cm^3 min^{-1} of methane. After 30 minutes the gas flow was changed back to 400 cm^3 min^{-1} of argon, and the setup was allowed to cool to room temperature. The samples were removed after the furnace had cooled below 200 °C.

2.2. Sample analysis

The samples were characterized using Raman spectroscopy with a Labram 300 microscope (Jobin Yvon, France) with excitation at 632.8 nm (13 mW, with collections typically 100 seconds). Samples were prepared for Raman analysis by dispersing some of the sample onto a silicon wafer.

Thermogravimetric analysis (TGA) was conducted using a thermobalance (TG762, Stanton Redcroft, UK) heating from room temperature to 1000°C at a rate of 10 °C min^{-1}. Samples were prepared for scanning electron microscopy (SEM) by placing them onto a piece of carbon tape (a carbon sticky) that was affixed to a specimen stub. SEM images were obtained using a XL30CP microscope (Philips, Netherlands) having the secondary electron detector with a typical working distance of 10 mm and accelerating voltage of 30 kV. Samples were prepared for transmission electron microscopy (TEM) by dispersing some of the material in ethanol using gentle ultrasonication and by dropping a little of the dispersed product onto carbon-coated grids. TEM images were captured using a JEM-1230 Electron Microscope (JEOL, Japan) with an accelerating voltage of 100 kV.

3. Results and discussion

Representative TEM images of the carbon nanotubes produced are shown in Fig.1, and corresponding SEM images are shown in Fig. 2. As can be seen, there is clear evidence for production of predominantly high-quality SWCNT, and these results are consistent with the Raman spectroscopy and TGA.

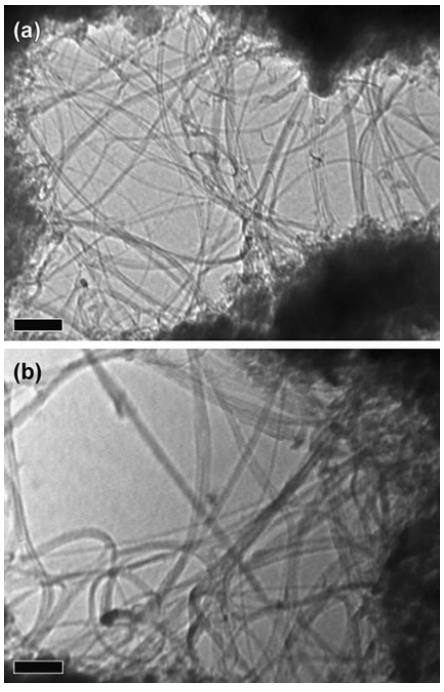

Fig. 1. TEM images [scale bar 50 nm] of the tubes grown (a) with the Mo10 catalyst, and (b) with the Ce10 catalyst. Both images show the presence of high-quality SWCNTs with extensive bundling between tubes.

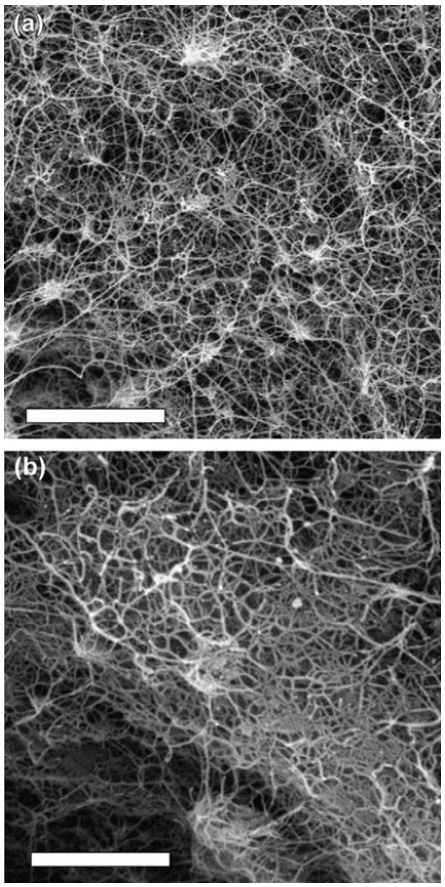

Fig. 2. SEM images [scale bars 2 μm] of the tubes grown (a) with the Mo10 catalyst, and (b) with the Ce10 catalyst. The images confirm the production of large quantities of carbon nanotubes.

The Raman spectra in general show peaks that are characteristic for graphitic resonances, see Fig. 3. As has been discussed in detail [17], the G band (at ~1590 cm^{-1}) originates from ordered, well-graphitized (sp^2) carbon bonding, while the D band (at ~1330 cm^{-1}) is the disorder-activated band and is indicative of non-graphitized (sp^3) carbon bonding. The Raman spectra also show low-frequency peaks (~150–250 cm^{-1}) that result from radial breathing modes (RBMs) that are unique to single-walled carbon nanotubes (SWCNTs). The frequencies of the RBMs are inversely proportional to the diameters of the tubes. The shoulder to the low-frequency side of the G band (at ~1550 cm^{-1}) is also indicative of the presence of SWCNTs [18]. The ratio of integrated areas of the D and G bands (D/G ratio) in the Raman spectrum has been used widely as a measure of the quality of graphitization of a sample, and therefore of the quality of the CNT produced: a smaller D/G ratio is consistent with fewer tube defects.

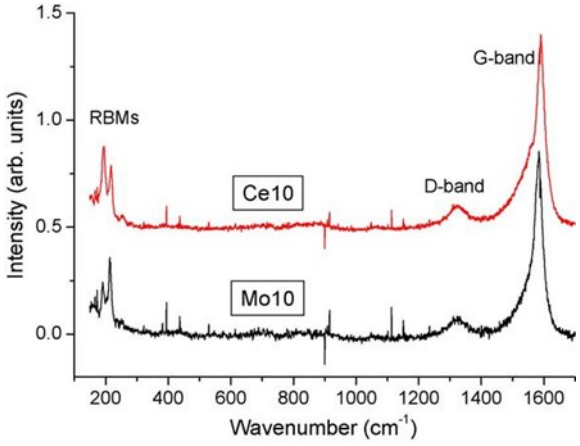

Fig. 3. Raman spectra obtained for samples Ce10 (upper trace) and Mo10 (lower trace). The radial-breathing modes (RBM) indicate the presence of SWCNT. The ratio of intensity of the D and G-bands (D/G ratio) indicates that the samples are well-graphitized.

The TGA of the products showed weight losses in the temperature range 440–600 °C, which is typical for as-prepared CNT samples. The total mass of C produced was calculated from the percentage ratio of C removed at high temperature in the TGA. The yields were found to be in the range 10.3 to 30.3 mg of C, showing that the catalysts are indeed very effective at producing CNT.

A summary of the results of the Raman spectroscopy and thermogravimetric analysis are shown in Table 2. The yield of C as determined by high temperature burn-off in the TGA indicates that good graphitic carbon has been produced. The high intensity of radial breathing modes from the Raman spectra (Fig. 3), along with the abundant tubes seen in the electron microscopy (Figs 1 and 2) give us confidence that the yields obtained represent closely the mass yields of carbon nanotubes. In terms of production of graphitic C, it can be seen that all of the catalysts are equally effective (~10–20 mg C yield): however, low loadings of Mo are particularly productive, as can be seen from the yields for samples Mo10 and Mo50. Despite the highest yield of the Mo50 catalyst (30.3 mg of C), the Raman spectroscopy reveals that the graphitic quality of the SWCNT (as indicated by the D/G ratio) for that sample is lower than some of the other catalyst combinations.

Sample	mg graphitic C obtained	D/G-band ratio	RBM detected?	Most intense RBM (cm^{-1})
Fe100	10.9	0.09	Yes	212
Mo100	12.2	0.78	No	–
Ce100	10.3	0.92	No	–
Ce10	14.2	0.10	Yes	188
Ce50	13.6	0.20	Yes	188
Ce90	13.6	0.81	Yes	188
Mo10	18.8	0.11	Yes	212
Mo50	30.3	0.17	Yes	212
Mo90	15.9	0.40	Yes	212

Table 2. Summary of the results of the Raman spectroscopy and thermogravimetric analysis. The sample labels correspond to the metal loadings shown in Table 1. The yield of graphitic C (in mg) is shown, along with the ratio of the integrated intensity of the D and G-bands of the Raman spectrum (D/G ratio). The observation, or not, of radial breathing mode (RBM) transitions in the Raman spectrum is a clear indicator for production of single-walled nanotubes. The right-hand column indicates the wavenumber of the most intense RBM observed, and is inversely related to the radius of the corresponding SWCNT.

We can see from Table 2, that Mo or Ce alone produces a totally ineffective catalyst, the D/G ratios are exceedingly poor, and no RBMs are observed: this indicates that there are no, or very few, SWCNTs. In terms of graphitic quality, the best CNTs were observed for Fe100, Mo10 and Ce10, and the D/G ratios for these are approximately the same. As the loading of Ce or Mo is increased relative to Fe, it is seen that the D/G ratio increases, indicating that the quality of the CNTs is decreasing, see Fig. 4. It is clear from the Ce10 and Mo10 results that addition of a small proportion of Mo or Ce is beneficial for increasing the carbon yield, without lowering the quality of the SWCNTs. The best catalysts are therefore the Ce10 and Mo10 catalysts. However, we stress that the CVD system has not been fully optimized in terms of the other parameters such as temperature, gas flow, buffer gas. Therefore, finer tuning of these parameters would potentially improve the yields for the Ce10 and Mo10 catalysts. For comparison, the D/G ratio of a commercial sample of SWCNTs (HiPco tubes, Carbon Nanotechnologies Inc., Houston, TX, USA) was measured, using the same method as outlined above, to be 0.12. Thus, the quality of the SWCNT reported here is very high.

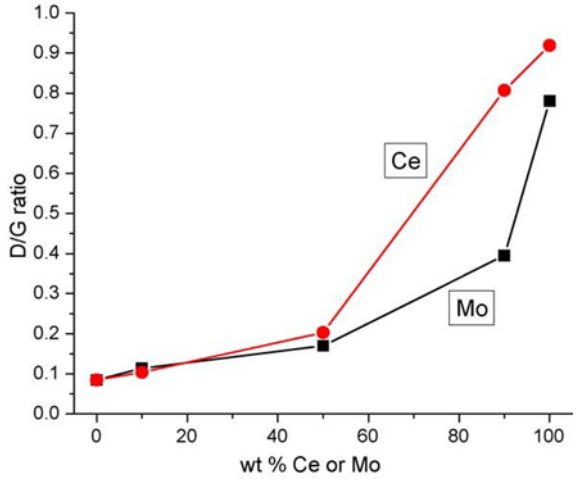

Fig. 4. Plot of the D/G ratio as a function of Mo or Ce loading. High values of the D/G ratio indicate poorer quality SWCNTs. The results show a monotonic decline in graphitic quality of the SWCNT as the fraction of Mo (Ce) to Fe is increased.

As discussed above, the use of Mo/Fe to enhance growth of SWCNTs has been well-documented [4]. On the other hand, Ce has received very little attention as a potential catalyst for SWCNT growth. Cerium oxide (CeO_2) has a reputation for use in environmental catalysis [19]. Liu et al. have looked at the combination of Ce/Ni doped into graphite rods used in an arc-discharge system for growth of SWCNTs, and have shown that Ce promotes growth of narrower diameter tubes [20]. We show here, for the first time, the use of Ce as a catalyst in SWCNT growth using CVD. It is interesting to consider that cerium is known as a catalyst in diesel-soot abatement technology [19], and it is evident that Ce alone, if anything, does not promote the growth of SWCNT. However, Ce does appear to make an effective bimetallic additive in combination with Fe for growth of SWCNTs. Ce is not known as a catalyst for promotion of dehydroaromatization (DHA) of methane. The fact that low loadings of Ce and Mo appear to be equally effective for promoting SWCNT growth goes against the hypothesis that Mo enables the *ring-addition mechanism* for growth of SWCNT. It seems more likely that Mo and Ce both promote the growth by assisting the metal nanoparticle to operate via the *decomposition mechanism*. In addition, our results question the special importance that has been attributed to Mo as an additive to Fe-based catalysts for SWCNT growth, as it appears that Ce is equally effective.

There is evidence to support that formation of the alloy $MgFe_2O_4$ is a key step in the CVD process using MgO-supported Fe catalysts [10,16]. Our results show that the presence of small loadings (~10%) of the additive Ce or Mo does not significantly interfere with this proposed mechanism, although we have no direct evidence to show that the Ce or Mo is participating in the alloy formation. Instead, it

appears that small loadings of Ce or Mo are able to enhance the CVD for growth of SWCNTs beyond the use of Fe alone.

A closer inspection of the Raman spectra shows systematic differences in the RBMs and in the shape of the G-bands. The RBMs for all samples show only two intense RBM peaks. For the Fe catalysts loaded with Ce, we find that the RBM at 188 cm^{-1} is always more intense than the RBM at 212 cm^{-1}. The frequency $(\omega_{RBM} / \mathrm{cm}^{-1})$ of a RBM of a SWCNT has been related empirically to the diameter (d_t / nm) of the tube [21],

$$d_t / \mathrm{nm} \approx \frac{248}{\omega_{RBM} / \mathrm{cm}^{-1}} \quad .(1)$$

Using this equation, we find that the RBM at 188 cm^{-1} corresponds to a tube with diameter of 1.32 nm, and that at 212 cm^{-1} corresponds to a tube with diameter of 1.17 nm. Examination of an appropriate Kataura plot suggests that both of these tubes are metallic [22]. Of course, there will be a range of tubes of other diameters in the sample: we only see two intense RBMs because we are using a single excitation wavelength (632.8 nm), and these are the tubes that show resonances close to this optical excitation energy.

The region of the G-band for samples Ce10 and Mo10 is shown expanded in Fig. 5. It can be seen that the G-band is much wider for the Ce10 sample than the Mo10 sample, which we attribute to differences in the distributions of chiralities of the nanotubes. The G-band region consists of two regions, a high-frequency band (ω^+), which can be fitted with a Lorentzian lineshape, and a low-frequency band (ω^-). The ω^- band can be decomposed into contributions from metallic and semiconducting SWCNTs. The semiconducting band $(\omega^-_{\mathrm{semi}})$ usually occurs ~50 cm^{-1} lower than ω^+ and is normally fitted with a Lorentzian lineshape. The metallic band $(\omega^-_{\mathrm{met}})$ is shifted ~80 cm^{-1} lower than ω^+ and is best fitted by a Breit–Wigner–Fano lineshape [17,23]. Using the data shown in Fig. 5, we have fitted the G-bands for both samples using a combination of the above lineshapes. The results are summarized in Table 3.

Sample	Area of peaks (normalized to the area of ω^+)		
	ω^-_{met}	ω^-_{semi}	$\omega^-_{\text{met}} / \omega^-_{\text{semi}}$
Ce10	0.29	0.31	0.93
Mo10	0.16	0.21	0.76

Table 3. Summary of results of fitting lineshapes to the G-band region of the Raman spectrum (excitation at 632.8 nm) for samples Ce10 and Mo10. The integrated intensities (areas) of the peaks attributed to metallic (ω^-_{met}) and semiconducting (ω^-_{semi}) SWCNTs have been normalized to the high-frequency (ω^+) component (see Fig. 4, and text for details). The ratios in the right-hand column indicate a higher proportion of metallic to semiconducting SWCNTs, within the limited subset of tubes that are detected at this excitation wavelength.

As can be seen from Fig. 5 and from Table 3, the cerium-loaded catalyst Ce10 produced a higher proportion (~25%) of metallic SWCNTs compared to the molybdenum-loaded Mo10 catalyst, within the subset of tubes that are detected at the particular optical excitation. Raman excitation at a number of different wavelengths would be required to determine if this preference for metallic tubes was true for the whole sample. However, we can say that there is a clear difference in the distributions of chiralities of the tubes for the two catalysts. The difference suggests that the mechanism for SWCNT growth may be different for the Ce versus Mo catalysts. The electronic properties of a SWCNT are intimately linked to its structure, and can be determined from the chiral (or Hamada) vector (*n*, *m*) of the nanotube [24]. If $(n-m)=3q$, where *q* is an integer, then the tube is metallic, otherwise it is semiconducting. For a random sample of tubes, it would be expected that around a third of the tubes would be metallic. In the present case, it can be seen that metallic tubes are more favoured than average, for both Ce and Mo catalysts. One of the future goals of SWCNT synthesis is to selectively produce nanotubes that favour predominantly metallic or semiconducting structures, so that these may be targeted for specific applications. Although such fine control in CVD appears very challenging, nevertheless we may use different catalysts to bias the quality and structure of SWCNT. As our understanding of the growth mechanism associated with different catalysts increases, we hope to be able to develop CVD catalysts that are both more efficient and more selective.

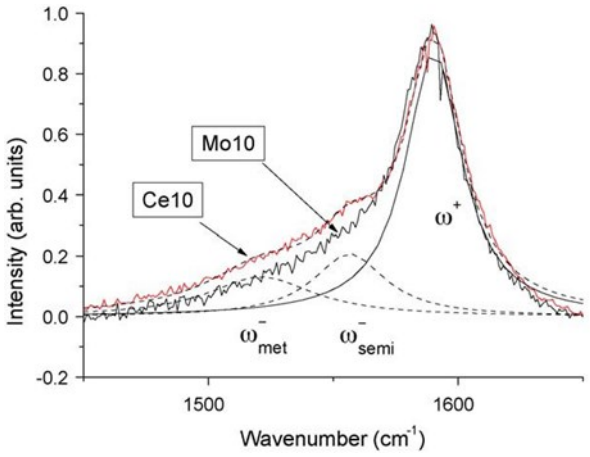

Fig. 5. Expanded G-band region of Raman spectra of Ce10 and Mo10 samples, showing fits of two Lorentzian and one Breit–Wigner–Fano curves to the G-band region of the Ce10 data. The spectra show a larger metallic peak $\omega^{-}_{\mathrm{met}}$ (~1520 cm^{-1}) for Ce10 than for Mo10. It should be noted that only a limited subset of the nanotubes are detected at this particular Raman excitation wavelength (632.8 nm).

5. Conclusions

In the present work we have studied the use of bimetallic Ce/Fe and Mo/Fe catalysts at various loadings on MgO supports. We have demonstrated for the first time, to the best of our knowledge, the use of Ce-based catalysts for CVD growth of carbon nanotubes. Our results suggest that the Ce/Fe system with relative loading of 10 wt % are very suitable for catalysts that favour single-walled carbon nanotube growth. We found that Ce and Mo are both equally good at improving growth of SWCNTs compared to Fe alone, suggesting that dehydroaromatization is not the defining mechanism for the growth, as has been suggested for Mo/Fe systems previously. Our results show that Ce and Mo do not seriously perturb the well-known Fe/MgO system for growth of high quality SWCNT. Using Raman spectroscopy, we have shown that the Ce(10%)/Fe/MgO catalyst system favours growth of metallic SWCNTs compared to the analogous Mo(10%)/Fe/MgO system.

References

[1] A. C. Dupuis, The catalyst in the CCVD of carbon nanotubes - a review. *Progress in Materials Science* 50 (2005) 929-961.

[2] A. Moisala, A.G. Nasibulin, E. I. Kauppinen, The role of metal nanoparticles in the catalytic production of single-walled carbon nanotubes - a review. *Journal of Physics-Condensed Matter* 15(2005) S3011-S3035.

[3] H. J.Dai, Carbon nanotubes: Synthesis, integration, and properties, *Accounts of Chemical Research* 35(2002**)** 1035-1044.

[4] A. M. Cassell, J. A. Raymakers, J. Kong, H. J. Dai, Large scale CVD synthesis of single-walled carbon nanotubes, *Journal of Physical Chemistry B* 103(1999) 6484-6492.

[5] R. B. Little, Mechanistic aspects of carbon nanotube nucleation and growth, *Journal of Cluster Science* 14 (2000) 135-185.

[6] E. V. Matus, I. Z. Ismagilov, O. B. Sukhova, V. I. Zaikovskii, L.T. Tsikoza, Z. R. Ismagilov, J. A. Moulijn, Study of methane dehydroaromatization on impregnated Mo/ZSM-5 catalysts and characterization of nanostructured molybdenum phases and carbonaceous deposits. *Industrial & Engineering Chemistry Research* 46(2007**)** 4063-4074.

[7] Y. J. Tian, Z. Hu, Y. Yang,V. Chen, W. J. Ji, Y. Chen, Thermal analysis-mass spectroscopy coupling as a powerful technique to study the growth of carbon nanotubes from benzene. *Chemical Physics Letters* 388(2004**)** 259-262.

[8] Y. J. Tian, Z. Hu, Y. Yang, X. Z. Wang, X. Chen, H. Xu, Q. Wu, W.J. Ji, Y. Chen, In situ TA-MS study of the six-membered-ring-based growth of carbon nanotubes with benzene precursor. *Journal of the American Chemical Society* 126 (2004)1180-1183.

[9] R. J. Andrews, Carbon nanotubes: synthesis and functionalization. PhD thesis, University of Edinburgh, Edinburgh, UK, (2006).

[10] Q. W. Li, H. Yan, Y. Cheng, J. Zhang, Z. F. Liu, A scalable CVD synthesis of high-purity single-walled carbon nanotubes with porous MgO as support material. *Journal of Materials Chemistry* 12(2002) 1179-1183.

[11] H. Ago, K. Nakamura, S. Imamura, M. Tsuji, Growth of double-wall carbon nanotubes with diameter-controlled iron oxide nanoparticles supported on MgO, *Chemical Physics Letters* 391(2004) 308-313.

[12] H. Ago, S. Imamura, T. Okazaki, T. Saitoj, M. Yumura, M. Tsuji, CVD growth of single-walled carbon nanotubes with narrow diameter distribution over Fe/MgO catalyst and their fluorescence spectroscopy, *Journal of Physical Chemistry B* 109 (2005) 10035-10041.

[13] E. Flahaut, A. Peigney, C. Laurent, A. Rousset, Synthesis of single-walled carbon nanotube-Co-MgO composite powders and extraction of the nanotubes. *Journal of Materials Chemistry* 10(2000**)** 249-252.

[14] H. Ago, K. Nakamura, N. Uehara, M. Tsuji, Roles of metal-support interaction in growth of single- and double-walled carbon nanotubes studied with diameter-controlled iron particles supported on MgO. *Journal of Physical Chemistry B***,** 108 (2004) 18908-18915.

[15] J. F. Colomer, C. Stephan,V. Lefrant, G. Van Tendeloo, I. Willems, Z. Konya, A. Fonseca, C. Laurent, J. B. Nagy, Large-scale synthesis of single-wall carbon nanotubes by catalytic chemical vapor deposition (CCVD) method, *Chemical Physics Letters,* 317(2000**)** 83-89.

[16] G. Q. Ning, F. Wei, Q. Wen, G. H. Luo, Y. Wang, Y. Jin, Improvement of Fe/MgO catalysts by calcination for the growth of single-and double-walled carbon nanotubes. *Journal of Physical Chemistry B* 110 (2006**)**1201-1205.

[17] M. S. Dresselhaus, G. Dresselhaus, A. Jorio, A. G. Souza, R. Saito, Raman spectroscopy on isolated single wall carbon nanotubes. *Carbon* 40 (2002**)** 2043-2061.

[18] W. Z. Qian, T. Liu, F. Wei, H. Y. Yuan, Quantitative Raman characterization of the mixed samples of the single and multi-wall carbon nanotubes. *Carbon* 41 (2003**)**1851-1854.

[19] Trovarelli A. *Catalysis by ceria and related materials*. Imperial College Press: London 2002; Vol. 2.

[20] B. B. Liu, T. Wagberg, E. Olsson, R. S. Yang, H. D. Li, S. L. Zhang, H. B. Yang, G.T. Zou, B. Sundqvist, Synthesis and characterization of single-walled nanotubes produced with Ce/Ni as catalysts. *Chemical Physics Letters* 320 (2000**)** 365-372.

[21] M. S. Dresselhaus, G. Dresselhaus, A. Jorio, A. G. Souza, M. A. Pimenta, R. Saito,

Single nanotube Raman spectroscopy. *Accounts of Chemical Research* 35 (2002**)** 1070-1078.

[22] A. Jorio, P. T. Araujo, S. K. Doorn, H Maruyama , H. Chacham, M. A. Pimenta, The Kataura plot over broad energy and diameter ranges. *Physica Status Solidi B* 243 (2006**)** 3117.

[23] R. J. Andrews, C. F. Smith, A. J. Alexander, Mechanism of carbon nanotube growth from camphor and camphor analogs by chemical vapor deposition. *Carbon* 44(2006**)** 341-347.

[24] R. Saito, G. Dresselhaus, M. S. Dresselhaus, *Physical properties of Carbon Nanotubes*. ed.; Imperial College Press: London, UK, 1998.